Annals of
Pure and Applied
Mathematics

Combined Effect of Hartmann and Rayleigh Numbers on Free Convective Flow in a Square Cavity with Different Positions of Heated Elliptic Obstacle

Abdul Halim Bhuiyan[1], Md. Nasir Uddin[2] and *M. A. Alim[3]*

[1]Department of Mathematics, Bangladesh University of Engineering and Technology Dhaka-1000, Bangladesh. E-mail: ahalim@math.buet.ac.bd

[2]Department of Mathematics, Bangladesh University of Engineering and Technology Dhaka-1000, Bangladesh. E-mail: mnasiruddin07@gmail.com

[3]Department of Mathematics, Bangladesh University of Engineering and Technology Dhaka-1000, Bangladesh. E-mail: maalim@math.buet.ac.bd

Abstract. This paper is concerned with the combined effect of Hartmann and Rayleigh numbers on the free convective flow in a square cavity with different positions of heated elliptic obstacle. The two-dimensional Physical and mathematical model have been developed, and mathematical model includes the system of governing mass, momentum and energy equations are solved by the finite element method. The calculations have been computed for Prandtl number Pr = 0.71, and the different values of Hartmann number and Rayleigh number. The results are illustrated with the streamlines, isotherms, velocity and temperature fields as well as local Nusselt number for different configurations.

Keywords: Hartmann number, Rayleigh number, free convection, square cavity, finite element method

AMS Mathematics Subject Classification (2010): 76Dxx, 76D99, 76E09

1. Introduction

One of the most important phenomena in thermal system is free convection; this is due to its wide applications in nature and engineering such as oceanic currents, sea-wind, fluid flows around shrouded heat dissipation fins, free air cooling without the aid of fans, electronics cooling, heat exchangers and so on. MHD natural convection flow and heat transfer in a laterally heated partitioned enclosure is investigated by Kahveci and Oztuna [1]. Taghikhani and Chavoshi [2] investigated two dimensional magnetohydrodynamics (MHD) free convection with internal heating in a square cavity and observed the effect of the magnetic field which is to reduce the convective heat transfer inside the cavity. Parvin and Nasrin [3] analyzed the flow and heat transfer characteristics for MHD free convection in an enclosure with a heated obstacle and found that, buoyancy-induced vortex in the streamlines increase as well as the thermal layer near the heated surface becomes thick with increasing Rayleigh number. Hossain and Alim [4] numerically investigated the two-dimensional laminar steady-state on MHD free convection with

trapezoidal cavity with uniformly heated bottom wall. Sathiyamoorty et al. [5] studied the steady natural convection flow in a square cavity with linearly heated side walls. Nawaf [6] investigated the natural convection in a square porous cavity with an oscillating wall temperature. The results are presented to demonstrate the temporal variation of the streamlines, the isotherms and the Nusselt number. The peak value of the average Nusselt number is observed to occur at the resonance nondimensional frequency of 450 in the range considered (1–2000) for Rayleigh number 103. Hakan et al. [7] analyzed the laminar MHD mixed convection flow in a top sided lid- driven cavity heated by corner heater and considered the temperature of the lid is lower than that of heater. Also Hakan et al. [8] studied the effects of volumetric heat sources on Natural convection in wavy-walled enclosures are studied numerically. Bakhshan and Ashoori [9] investigated the analysis of a fluid behavior in a rectangular enclosure under the effect of magnetic field. They observed that Nusselt number rises with increasing Grashof and Prandtl numbers and decreasing Hartmann and orientation of magnetic field.

Therefore, in the light of above literatures, the aim of the present work is to investigate the combined effect of Hartmann and Rayleigh numbers on free convective flow in a square cavity with different positions of heated elliptic obstacle.

2. Model and mathematical formulation

Figure 1 shows a schematic diagram and the coordinates of a two-dimensional square cavity, where the right wall is maintained at a uniform temperature T_h and other walls maintained cooled temperature T_c. A heated elliptic obstacle is considered in a square cavity with different positions. The fluid is permeated by a uniform magnetic field B_0 which is applied normal to the direction of the flow and the gravitational force (g) acts in the vertically downward direction. The fluid properties, including the electrical conductivity, are considered to be constant, except for the density, so that the Boussinesq approximation is used. Neglecting the radiation mode of the heat transfer and Joule heating, the governing equations for mass, momentum and energy of a steady tow-dimensional natural convection flow in a square cavity are as follows:
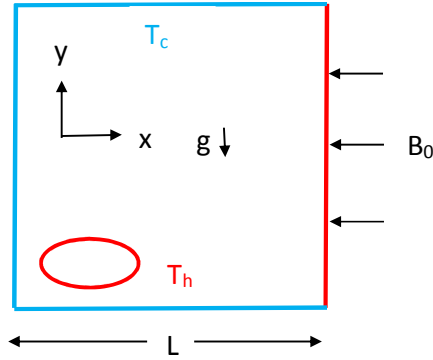
Figure 1: The flow configuration and coordinate system

$$\frac{\partial u}{\partial x} + \frac{\partial v}{\partial y} = 0 \tag{1}$$

$$\rho\left(u\frac{\partial u}{\partial x} + v\frac{\partial u}{\partial y}\right) = -\frac{\partial p}{\partial x} + \mu\left(\frac{\partial^2 u}{\partial x^2} + \frac{\partial^2 u}{\partial y^2}\right) \tag{2}$$

$$\rho\left(u\frac{\partial v}{\partial x} + v\frac{\partial v}{\partial y}\right) = -\frac{\partial p}{\partial y} + \mu\left(\frac{\partial^2 v}{\partial x^2} + \frac{\partial^2 v}{\partial y^2}\right) + \rho g\beta\left(T - T_c\right) - \sigma B_0^2 v \tag{3}$$

$$u\frac{\partial T}{\partial x}+v\frac{\partial T}{\partial y}= \alpha\left(\frac{\partial^2 T}{\partial x^2}+\frac{\partial^2 T}{\partial y^2}\right) \tag{4}$$

The governing equations are nondimensionalized using the following dimensionless variables:

$$X=\frac{x}{L},\quad Y=\frac{y}{L},\quad U=\frac{uL}{\alpha},\quad V=\frac{vL}{\alpha},\quad P=\frac{pL^2}{\rho\alpha^2},\quad \theta=\frac{T-T_c}{T_h-T_c}\ ,$$

$$\sigma=\frac{\rho^2\alpha}{L^2},\quad \alpha=\frac{k}{\rho C_p}$$

Introducing the above dimensionless variables, the following dimensionless forms of the governing equations are obtained as follows:

$$\frac{\partial U}{\partial X}+\frac{\partial V}{\partial Y}=0. \tag{5}$$

$$U\frac{\partial U}{\partial X}+V\frac{\partial U}{\partial Y}=-\frac{\partial P}{\partial X}+\Pr\left(\frac{\partial^2 U}{\partial X^2}+\frac{\partial^2 U}{\partial Y^2}\right). \tag{6}$$

$$U\frac{\partial V}{\partial X}+V\frac{\partial V}{\partial Y}=-\frac{\partial P}{\partial Y}+\Pr\left(\frac{\partial^2 V}{\partial X^2}+\frac{\partial^2 V}{\partial Y^2}\right)+Ra\Pr\theta\ -\ Ha^2\Pr V. \tag{7}$$

$$U\frac{\partial\theta}{\partial X}+V\frac{\partial\theta}{\partial Y}= \frac{\partial^2\theta}{\partial X^2}+\frac{\partial^2\theta}{\partial Y^2}. \tag{8}$$

Here Pr is the Prandtl number, Ra is the Rayleigh number and Ha is the Hartmann number, which are defined as:

$$\Pr=\frac{v}{\alpha},\ Ha^2=\frac{\sigma B_0^2 L^2}{\mu}\ ,Ra=\frac{g\beta L^3\left(T_h-T_c\right)\Pr}{v^2}\ .$$

The corresponding boundary conditions then take the following form:

$U=V=0,\ \theta=1\left(\text{at right wall of the cavity and heated elliptic obstacle}\right)$

$U=V=0, \theta=0\,(\text{at other walls})$

$P=0\left(\text{fluid pressure, at the inside and on the wall of the enclosure}\right)$

To computation of the rate of heat transfer, as local Nusselt number along the line $Y=0.5$ is used as follows:

$$Nu_{local}=-\left.\frac{\partial\theta}{\partial Y}\right|_{Y=0.5}$$

3. Numerical procedure

The Galerkin weighted residual method of finite element formulation is used to solve the dimensionless governing equations with the boundary conditions. This technique is well described by Taylor et al. [10] and Dechaumphai [11]. In this method, the solution domain is discretized into finite element meshes and then the nonlinear governing equations are transferred into a system of integral equations by applying the Galerkin

weighted residual method. Gauss quadrature method is used to perform the integration involved in each term of these equations. The nonlinear algebraic equations which are obtained are modified by imposition of boundary conditions and Newton's method is used to transform these modified equations into linear algebraic equations, and then these linear equations are solved by applying the triangular factorization method.

4. Code validation

In order to verify the accuracy of the numerical results which are obtained throughout the present study are compared with the previously published results. The present results of streamlines and isotherms are compared with that of Jani et al. [12] while Pr = 0.71, and obtained good agreement which is shown in Fig. 2.

Present work   Jani et al.[12]

Figure 2 (a): Comparison of the obtained results for streamlines with those from the open literature Jani et al. [12] while Ha=0 and Ha=100 with fixed Ra=10^5

Present work   Jani et al.[12]

Figure 2(b): Comparison of the obtained results for isotherms with those from the open literature Jani et al. [12] while Ha=0, Ha=50 and Ha=100 with fixed Ra=10^5

4. Results and discussion

In this paper, the numerical results has been performed to investigate the effects of various cavity configurations on the flow field while the values of Ra (= 10^4, 10^5 and 10^6) and Pr (= 0.71). The influence of the Hartmann number Ha (Ha = 0, 20, 50 and 100) with Ra = 10^4 on streamlines and isotherms are presented in Fig. 3 and Fig. 4 respectively, for bottom left configuration (BLC). From Fig. 3(a), it is seen that, in absence of Hartmann number, one cell is formed inside the cavity. With increasing of Hartmann number, the flow strength of the flow field decreases and the streamlines close

to the heated elliptic obstacle, which are observed in Figs. 3(b) - 3(d). The behaviors of the isotherms are illustrated in Figs. 4(a) – 4(d). The thermal boundary layer is found to increase but reduces the bend of the thermal boundary layer with the increase of Hartmann number. Moreover, the temperature of the flow field increases due to increase of Hartmann number Ha. The impacts of the Hartmann number Ha ($Ha = 0, 20, 50$ and 100) with $Ra = 10^5$, on streamlines and isotherms are presented in Fig. 5 and Fig. 6

Figure 3: Streamlines for (a) $Ha=0$; (b) $Ha=20$; (c) $Ha=50$; (d) $Ha=100$ while $Ra=10^4$ for BLC

respectively, for bottom left configuration (BLC). From Fig. 5(a), it is observed that, in absence of Hartmann number, two cells are formed inside the cavity, one cell is formed upper side in the cavity and other cell is formed near the bottom wall of the cavity. With increasing of Hartmann number, the streamlines close to the walls of the cavity and the fluid velocity decreases, which are observed in Figs. 5(b) - 5(d). As observations of the isotherms in Figs. 6(a) – 6(d), the thermal boundary layer increases and becomes like as linear with the increase of Hartmann number. Moreover, the temperature of the flow field increases due to increase of Hartmann number Ha. The behavior of streamlines and isotherms are presented in Fig. 7 and Fig. 8 respectively, for bottom left configuration (BLC) for the Hartmann number Ha ($Ha = 0, 20, 50$ and 100) with $Ra = 106$. From Fig. 7(a), it is seen that, in absence of Hartmann number, one cell is formed upper side in the cavity. With increasing of Hartmann number, the bend of the streamlines near the bottom wall increases, as a results the fluid velocity decreases, which are observed in Figs. 7(b) - 7(d). As seen the isotherms in Figs. 8(a) – 8(d), the thermal boundary layer increases but reduces the bend of the thermal boundary layer with the increase of Hartmann number.

Abdul Halim Bhuiyan, Md. Nasir Uddin and M. A. Alim

Moreover, the temperature of the flow field increases due to increase of Hartmann number Ha. The influence of the Hartmann number *Ha* (*Ha* = 0, 20, 50 and 100) on streamlines and isotherms are presented in Fig. 9 and Fig. 10 respectively, for top right configuration (TRC) while *Ra* = 10^4. From Fig. 9(a), it is seen that, in absence of Hartmann number, one cell is formed inside the cavity. As increase of magnetic field, the Hartmann number increases, as a results the flow strength decreases and the streamlines close to the heated elliptic obstacle, which are observed in Figs. 9(b) - 9(d). As observations of the isotherms in Figs. 10(a) – 10(d), the thermal boundary layer thickness increases with the increase of Hartmann number. Moreover, the temperature of the flow

Figure 4: Isotherms for (a) *Ha*=0; (b) *Ha*=20; (c) *Ha*=50; (d) *Ha*=100 while *Ra*=10^4 for BLC

field increases due to increase of Hartmann number *Ha*. Variation of streamlines and isotherms inside the cavity with Hartmann number *Ha* (*Ha* = 0, 20, 50 and 100) are presented in Fig. 11 and Fig. 12 respectively, for top right configuration (TRC) while *Ra* = 10^5. From Fig. 11(a), it is seen that, in absence of Hartmann number, one cell is formed inside the cavity. With increasing of Hartmann number, the flow strength decreases and the streamlines close to the heated elliptic obstacle, which are observed in Figs. 11(b) - 11(d). As seen the isotherms in Figs. 12(a) – 12(d), the thermal boundary layer is thicker and lesser bend of the isotherm lines is found for increasing of Hartmann number. Also the isotherm lines concentrate near the above the heated elliptic obstacle and near the right wall without effect of magnetic field while reduces the concentration of the isotherms with the increase of Hartmann number. The influence of the Hartmann number *Ha* (*Ha* = 0, 20, 50 and 100) on streamlines and isotherms are presented in Fig. 13 and Fig. 14 respectively, for top right configuration (TRC) while *Ra* = 10^6. From Fig. 13(a), it is seen that, in absence of Hartmann number, one cell is formed inside the cavity. With

increasing of Hartmann number, reduces the bend of the steam lines, as results the flow strength decreases that are observed in Figs. 13(b) - 13(d).

Figure 5: Streamlines for (a) *Ha*=0; (b) *Ha*=20; (c) *Ha*=50; (d) *Ha*=100 while *Ra*=10^5 for BLC

Figure 6: Isotherms for (a) *Ha*=0; (b) *Ha*=20; (c) *Ha*=50; (d) *Ha*=100 while *Ra*=10^5 for BLC

Abdul Halim Bhuiyan, Md. Nasir Uddin and M. A. Alim

Figure 7: Streamlines for (a) Ha=0; (b) Ha=20; (c) Ha=50; (d) Ha=100 while Ra=10^6 for BLC

Figure 8: Isotherms for (a) Ha=0; (b) Ha=20; (c) Ha=50; (d) Ha=100 while Ra=10^6 for BLC

Combined Effect of Hartmann and Rayleigh Numbers on Free Convective Flow
in a Square Cavity with Different Positions of Heated Elliptic Obstacle

Figure 9: Streamlines for (a) Ha=0; (b) Ha=20; (c) Ha=50; (d) Ha=100 while Ra=10^4 for TRC

Figure 10: Isotherms for (a) Ha=0; (b) Ha=20; (c) Ha=50; (d) Ha=100 while Ra=10^4 for TRC

Figure 11: Streamlines for (a) *Ha*=0; (b) *Ha*=20; (c) *Ha*=50; (d) *Ha*=100 while *Ra*=10^5 for TRC

Figure 12: Isotherms for (a) *Ha*=0; (b) *Ha*=20; (c) *Ha*=50; (d) *Ha*=100 while *Ra*=10^5 for TRC

Combined Effect of Hartmann and Rayleigh Numbers on Free Convective Flow
in a Square Cavity with Different Positions of Heated Elliptic Obstacle

Figure 13: Streamlines for (a) *Ha*=0; (b) *Ha*=20; (c) *Ha*=50; (d) *Ha*=100 while *Ra*=10^6 for TRC

Figure 14: Isotherms for (a) *Ha*=0; (b) *Ha*=20; (c) *Ha*=50; (d) *Ha*=100 while *Ra*=10^6 for TRC

Abdul Halim Bhuiyan, Md. Nasir Uddin and M. A. Alim

Figure 15: Velocity profiles for (a) $Ra=10^4$; (b) $Ra=10^5$; (c) $Ra=10^6$ along the line $Y = 0.5$ for BLC

Figure 16: Velocity profiles for (a) $Ra=10^4$; (b) $Ra=10^5$; (c) $Ra=10^6$ along the line $Y = 0.5$ for TRC

Figure 17: Temperature profiles for (a) $Ra=10^4$; (b) $Ra=10^5$; (c) $Ra=10^6$ along the line $Y = 0.5$ for BLC

Figure 18: Temperature profiles for (a) $Ra=10^4$; (b) $Ra=10^5$; (c) $Ra=10^6$ along the line $Y = 0.5$ for TRC

Abdul Halim Bhuiyan, Md. Nasir Uddin and M. A. Alim

Figure 19: Local Nusselt number for (a) Ra=10^4; (b) Ra=10^5; (c) Ra=10^6 along the line $Y = 0.5$ for BLC

Figure 20: Local Nusselt number for (a) Ra=10^4; (b) Ra=10^5; (c) Ra=10^6 along the line $Y = 0.5$ for TRC

As seen the isotherms in Figs. 14(a) – 14(d), the thermal boundary layer increases but reduces the bend of the thermal boundary layer with the increase of Hartmann number. Figure 15 presents the effects of Hartmann number Ha on the flow field as velocity profiles for bottom left configurations along the line $Y = 0.5$. As seen from the Fig. 15(a) for $Ra = 10^4$, the velocity decreases with the increase of Hartmann number above the middle of the cavity, but the velocity increases with the increase of Hartmann number below the middle of the cavity. This Fig. indicates that the velocity field becomes maximum and minimum points with $Ha = 0$, which are observed due to clockwise and counterclockwise flow directions. Similar results shows for TRC configurations, as observed in Figs. 16(a)-16(c). The temperature fields versus the coordinate of X directions are plotted in Fig. 17 for different Hartmann number with Ra. As seen from the Fig. 17 for $Ra = 10^4$, absence of Hartmann number, the maximum and minimum temperature are obtained. In presence of increasing Ra, the temperature field changes significantly. For TRC, the temperature field changes significantly with the increase of Hartmann number, which are observed in Figs. 18(a)-18(c). The local Nusselt numbers for variation of Hartmann number with Ra are presented in Figs. 19(a)-19(c). From these Figs., it is seen that the local Nusselt number decreases with the increase of Hartmann number. But, the local Nusselt number changes significantly, as observed in Figs. 20(a)-20(c).

5. Conclusion

Heat transfer by free convection of heated elliptic obstacle in a square cavity with uniform magnetic field B_0, which is applied normal to the direction of the flow, was studied numerically. The conservation of mass, momentum and energy equations were solved using the Galerkin weighted residual method of finite element formulation. As indicated above that the governing parameters were the Prandtl number Pr, the Rayleigh number Ra and the Hartmann number Ha. The effects of Hartmann number Ha due to heated elliptic obstacle, Prandtl number Pr and Rayleigh number Ra on the flow and temperature field have been studied in detail. From the present investigation the following conclusions may be drawn: if the Hartman number increases, the local Nusselt number decreases for BLC, but changes randomly for TRC.

REFERENCES

1. K.Kahveci and S.Oztuna, MHD natural convection flow and heat transfer in a laterally heated partitioned enclosure, *European J. Mechanics*, 28 (2009) 744.
2. M.ATaghikhani and H.R.Chavoshi, Two dimensional MHD free convection with internal heating in a square cavity, *Thermal Energy and Power Engineering*, 2 (2013) 22-28.
3. S. Parvin and R. Nasrin, Analysis of the flow and heat transfer characteristics for MHD free convection in an enclosure with a heated obstacle, *Nonlinear Analysis: Modeling and Control*, 16(1) (2009) 89–99.

4. M.S. Hossain and M.A. Ailm, MHD free convection with trapezoidal cavity with uniformly heated bottom wall, *Annals of Pure and Applied Mathematics*, 3(1) (2013) 41-55.
5. M. Sathiyamoorty, T.Basak and S.Roy, Steady Natural convection flow in a square cavity with linearly heated side walls, *International Journal of Heat and Mass Transfer*, 50 (2007) 766.
6. H. Saeid Nawaf, Natural convection in a square porous cavity with an oscillating wall temperature, *The Arabian Journal for Science and Engineering*, 61(1B) (April 2006).
7. F.O.Hakan, K.Al-Salem and L.Pop, MHD mixed convection in a lid-driven cavity with corner heater, *International Journal of Heat and Mass Transfer*, 54 (2011) 3494-3504.
8. F.O.Hakan, A.Eiyad, V.Yasin and C.Ali, Natural convection in wavy enclosures with volumetric heat sources, *International Journal of Thermal Sciences*, 50 (2011) 502-514.
9. Y. Bakhshan and H. Ashoori, Analysis of a fluid behavior in a rectangular enclosure under the effect ofmagnetic field, *World Academy of Science, Engineering and Technology*, 61 (2012) 637-641.
10. C. Taylor and P. Hood, A numerical solution of the Navier-Stokes equations using finite element technique, *Computer and Fluids*, 1(1) (1973) 73-89.
11. P.Dechaumphai, *Finite Element Method in Engineering*, 2ed, Chulalongkorn University Press, Bangkok, 1999.
12. S. Jani, M. Mahmoodi and M. Amini, Magnetohydrodynamic free convection in a square cavity from below and cooled other walls, *International Journal of Mechanical, Industrial Science and Engineering*, 7(4) (2013) 217-222.